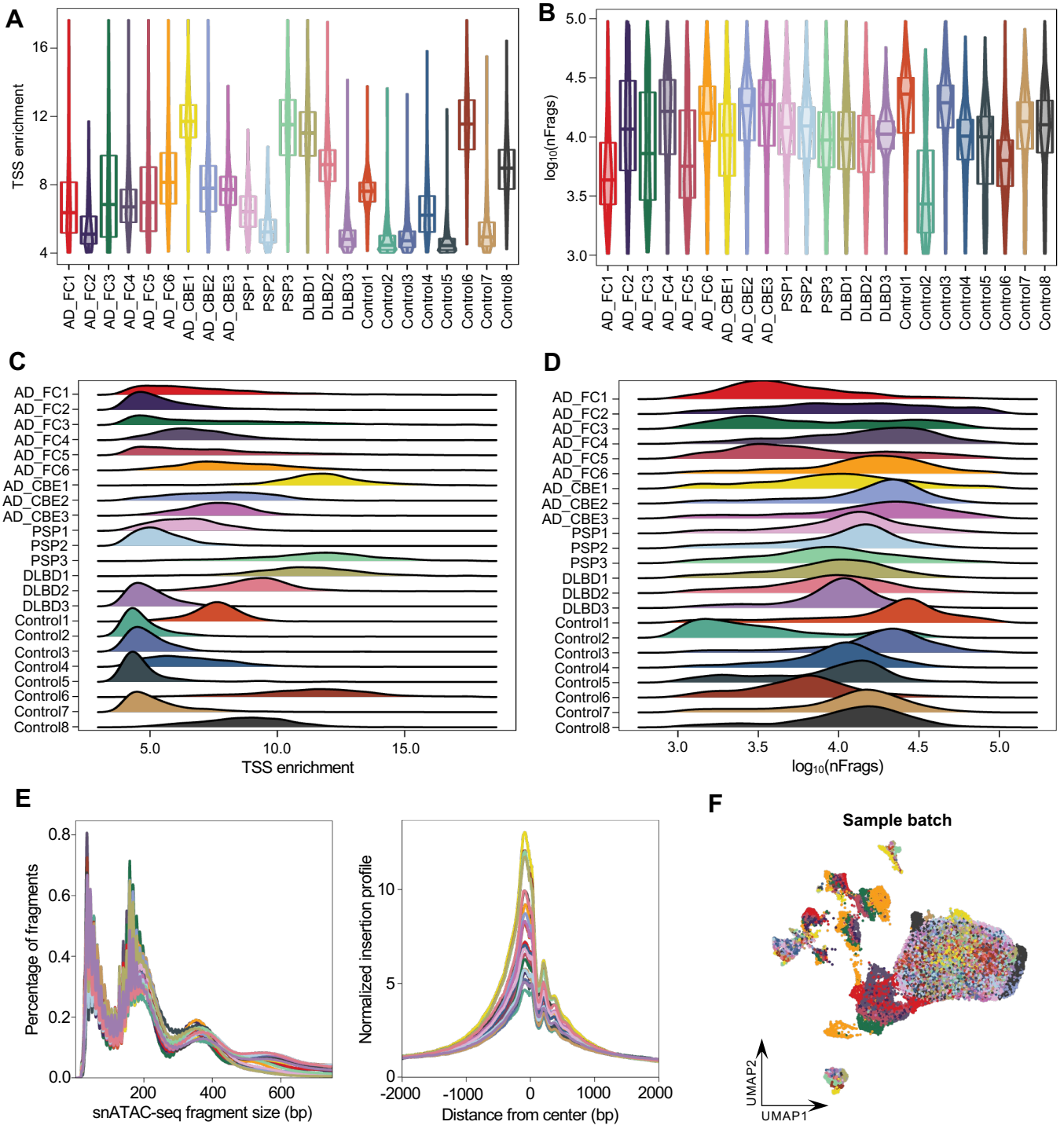

Figure S1. Single-nucleus multiome quality control matrix, Related to Figure 1. (**A**, **B**) Violin plots depicting the TSS enrichment score per nucleus (**A**) and number of detected ATAC fragments per nucleus (**B**). (**C**, **D**) Ridge plot for each sample for the TSS enrichment scores (**C**) and number of detected ATAC fragments per nucleus (**D**). (**E**) snATAC-seq fragment size distributions of all samples and TSS enrichment profiles. (**F**) Joint UMAP colored by sample batch.

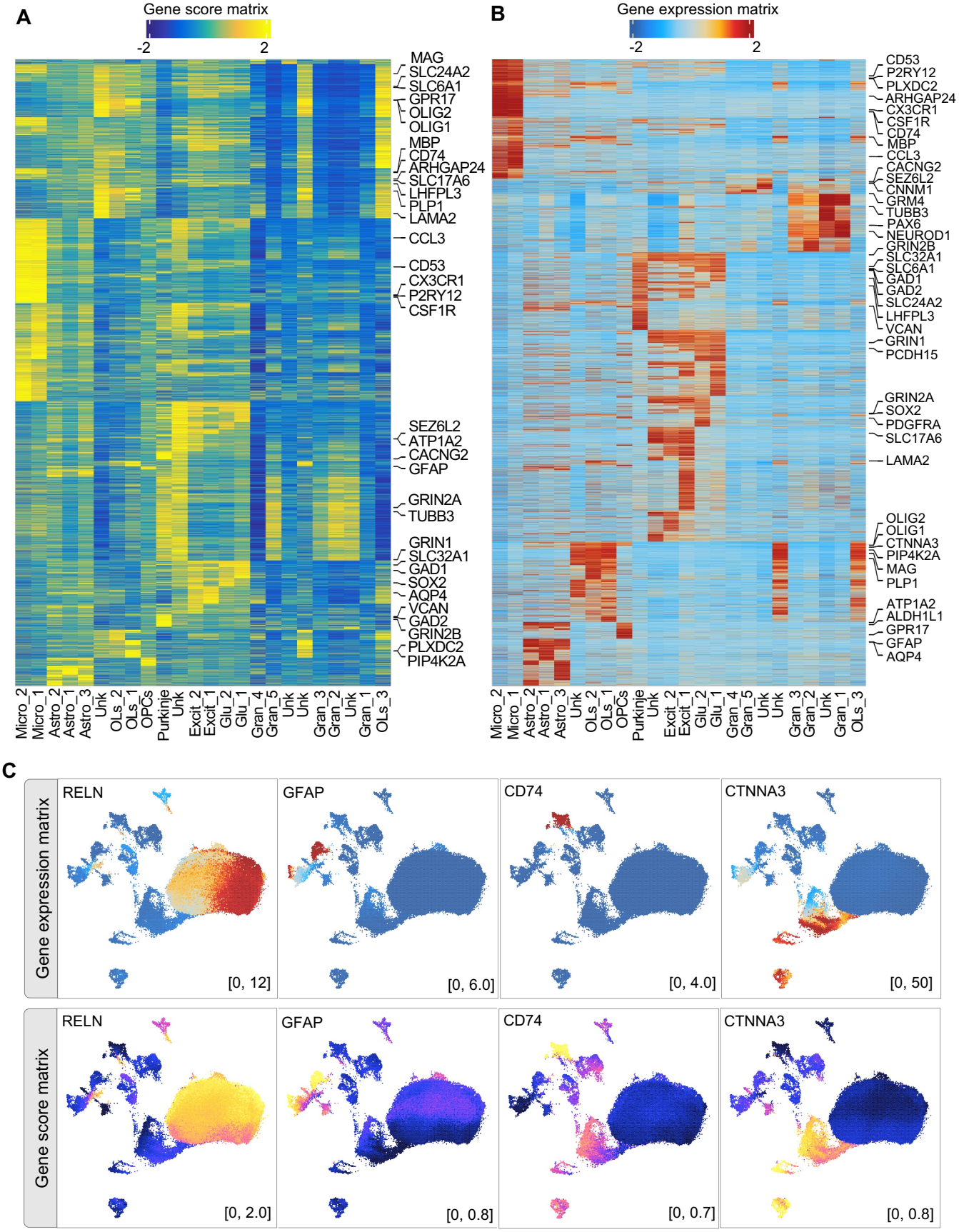

Figure S2. Selected cell type-specific marker genes, Related to Figure 1. (**A**, **B**) Heatmap depicting gene activity score (**A**) and gene expression (**B**) of selected cell type-specific marker genes. (**C**) Joint UMAPs for selected marker genes colored by normalized gene expression and gene activity scores.

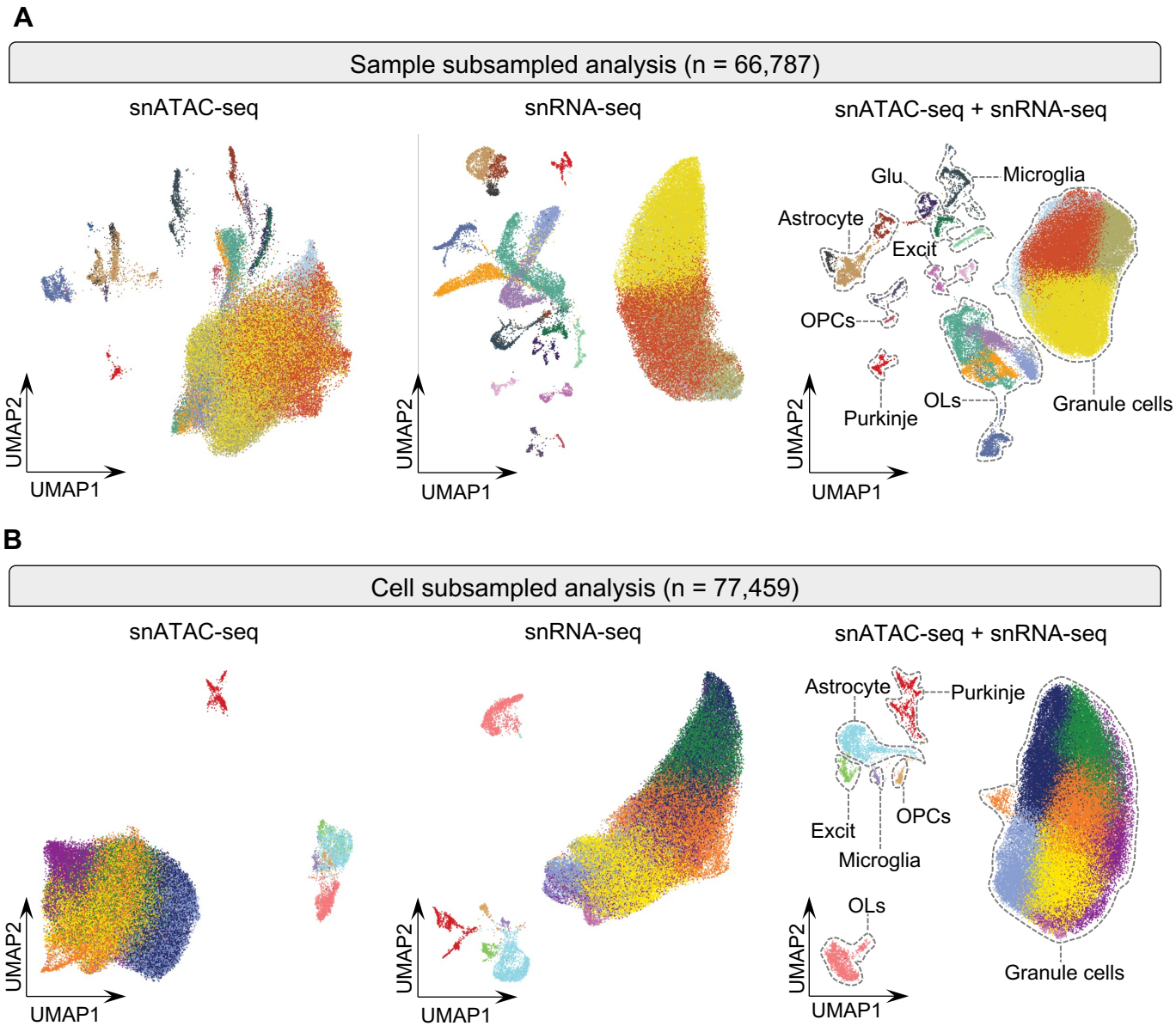

Figure S3. Clustering of scMultiome data robustness to subsampling analysis, Related to Figure 1 . (**A**) Repeated dimensionality reduction and clustering of the scMultiome datasets with eight samples (AD_FC4, AD_FC6, AD_CBE1, PSP1, DLBD1, Control1, Control5 and Control8) removed from the full dataset. UMAP representations of the full subsampled dataset using scATAC-seq, scRNA-seq and the scMultiome data. (**B**) Repeated dimensionality reduction and clustering of the scMultiome datasets with 25% of the cells randomly removed from the full dataset. UMAP representations of the full subsampled dataset using scATAC-seq, scRNA-seq and the scMultiome data. We used the same marker genes with **Figures 1D** and **1E** to identify cell subtypes.

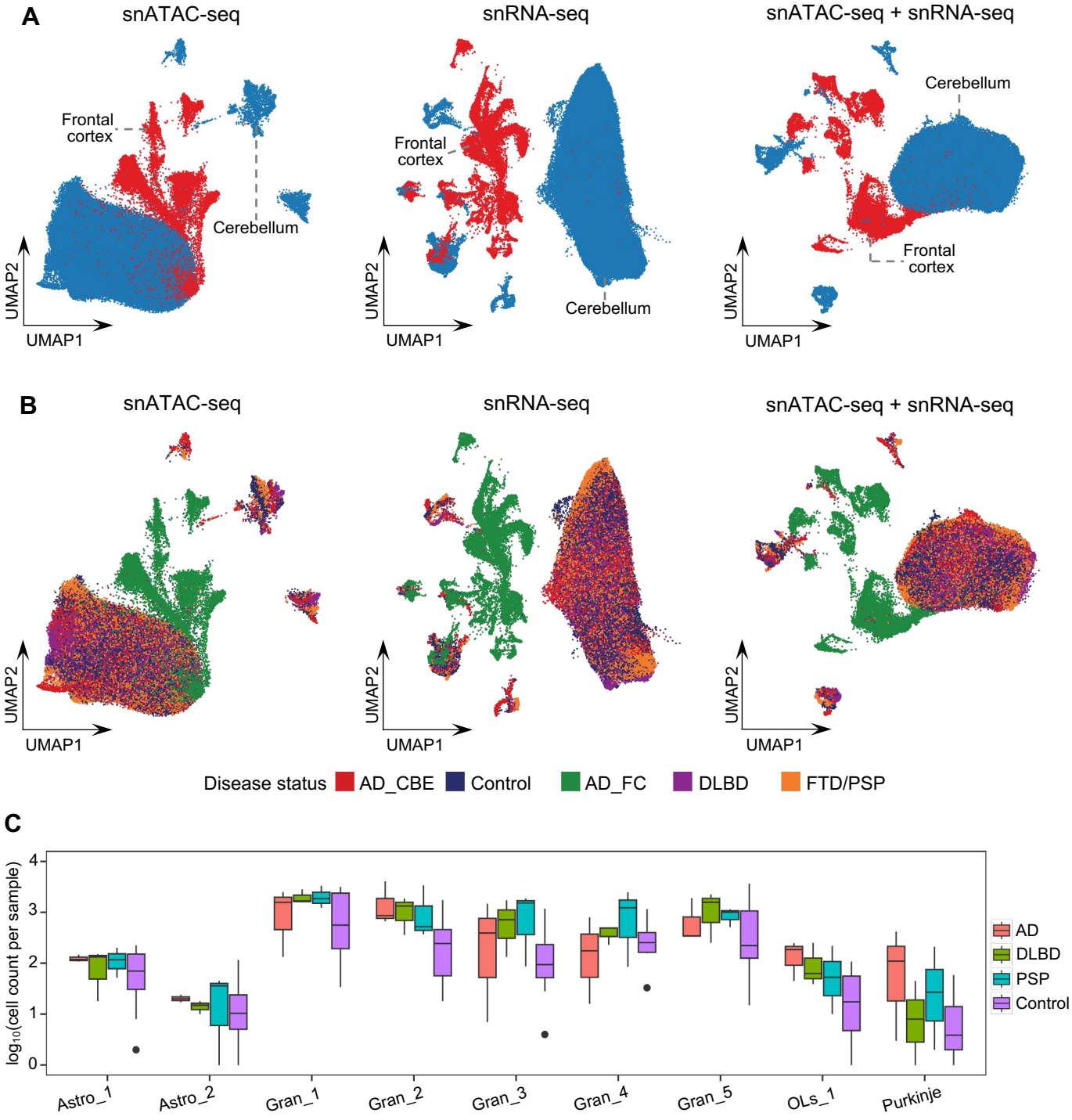

Figure S4. Cellular proportion of nucleus mapping to each cluster of each sample, split by brain regions and disease context, Related to Figure 1. (**A**) UMAP visualization where dots correspond to individual nuclei for snATAC-seq, snRNA-seq, and joint snATAC-seq and snRNA-seq, colored by brain regions. (**B**) UMAP visualization where dots correspond to individual nuclei for snATAC-seq, snRNA-seq, and joint snATAC-seq and snRNA-seq, colored by disease context. (**C**) Box plots showing the proportion of nucleus mapping to each cluster of each sample, split by disease context. Measures of significance were calculated using Kruskal-wallis rank sum test in R.

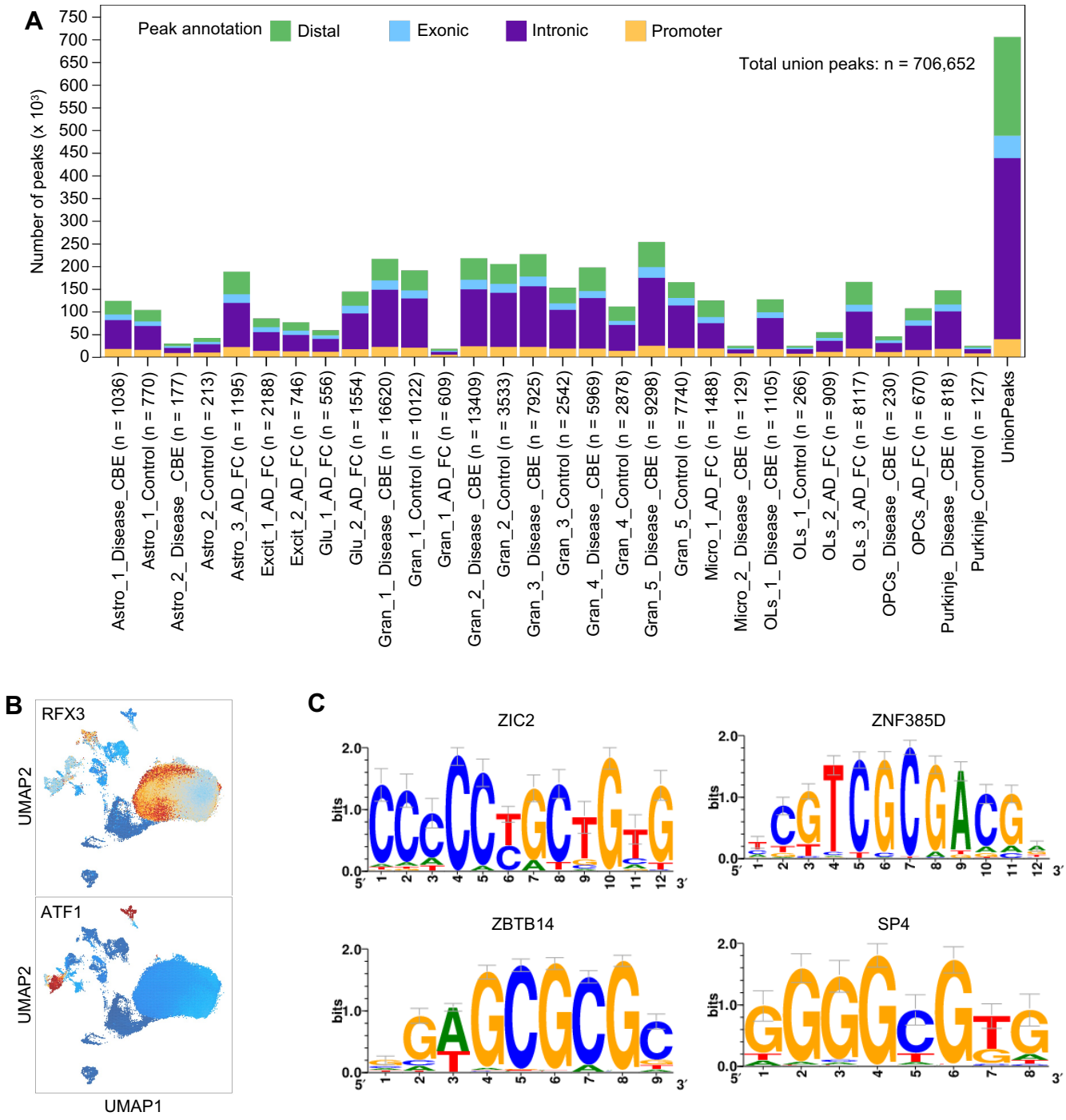

Figure S5. Chromatin accessibility profiles from snMultiome profiles of human cerebellum and frontal cortex reveal cell type-specific epigenetic landscapes, Related to Figure 2. (**A**) Number of chromatin accessibility peaks for each cell subtypes identified using snATAC-seq data. Peaks were required to be present in at least two pseudo-bulk ATAC replicates. (**B**) UMAPs of motif deviation scores for selected TFs enriched in granule cells (*RFX3*) and Purkinje cells (*ATF1*). (**C**) The candidate *cis*-regulatory elements enriched binding motifs of key transcription factors.

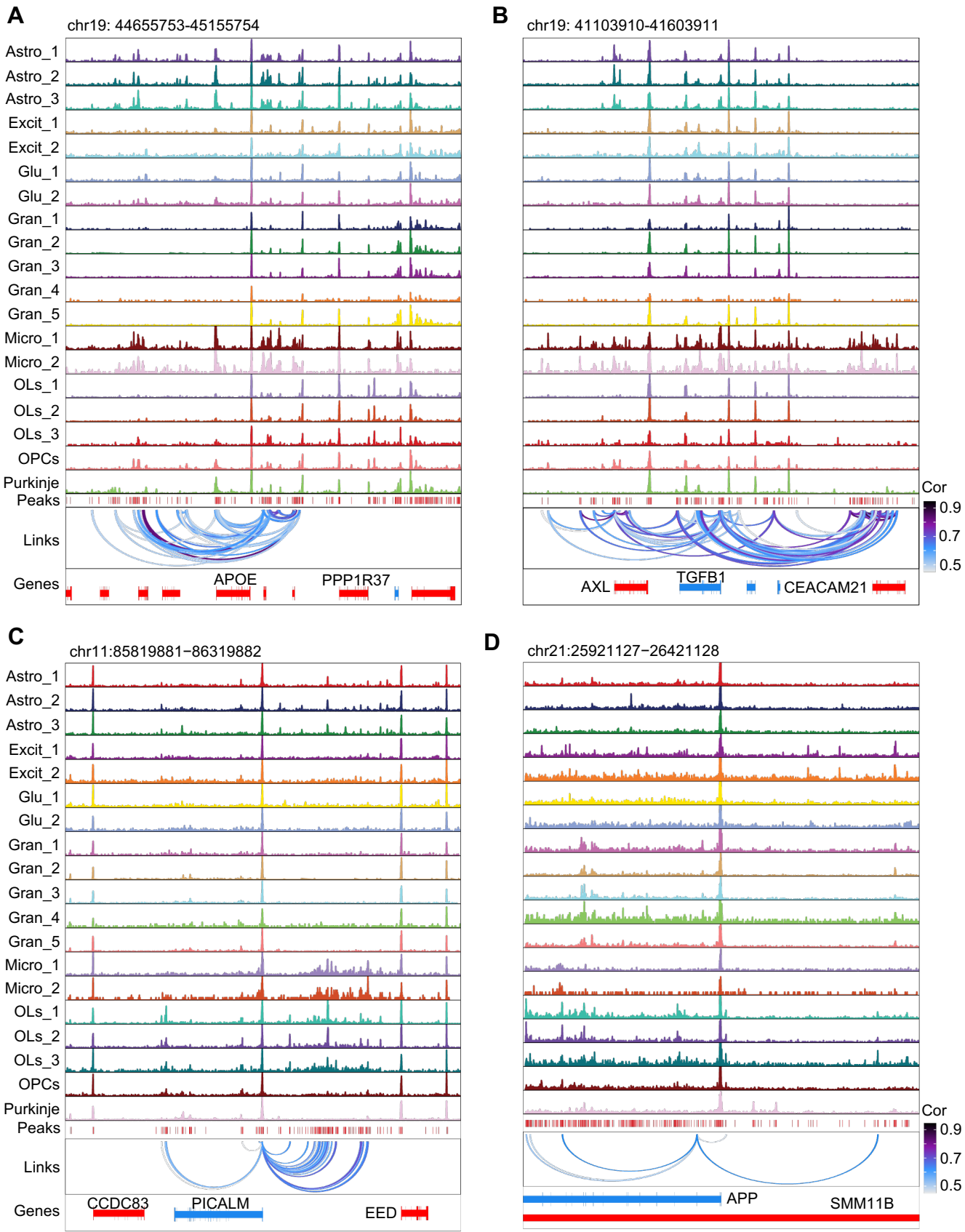

Figure S6. Identification of candidate *cis*-regulatory elements, Related to Figure 2. Genomic tracks for chromatin accessibility around 250 Kb flanking regions of *APOE* locus (**A**), *TGFB2* (**B**), *PICALM* (**C**) and *APP* (**D**). Peak-to-gene linkages were shown as loops below those genomic tracks and colored by linked correlation value.

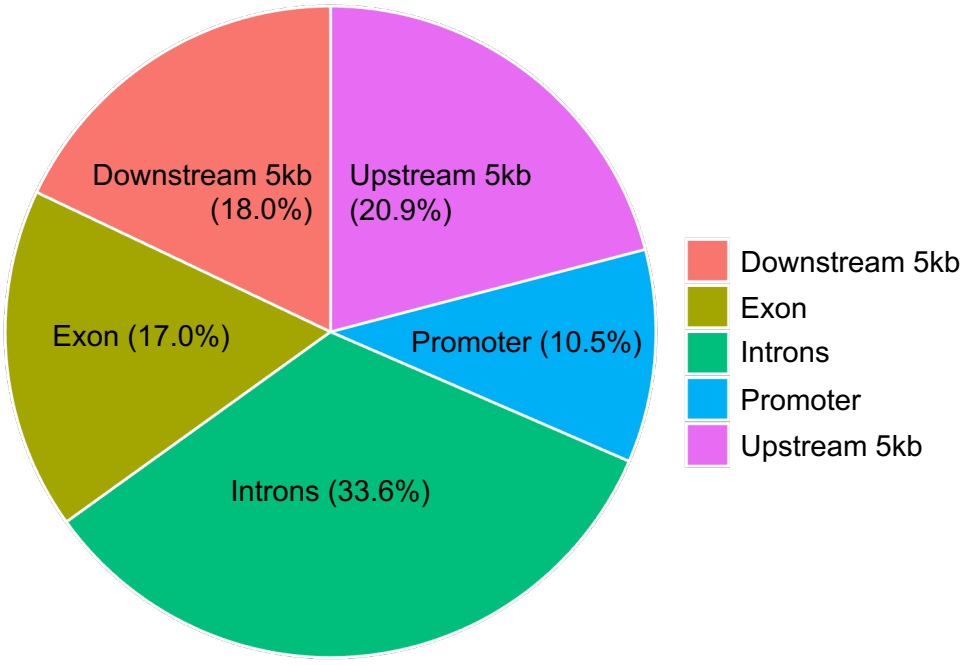

Figure S7. Pie charts showing percentage of candidate *cis*-regulatory elements in different functional genomic elements, including promoters, exons, introns, upstream 5 kb region of transcriptional start sites, and downstream 5 kb region of transcriptional start sites, Related to Figure 2.

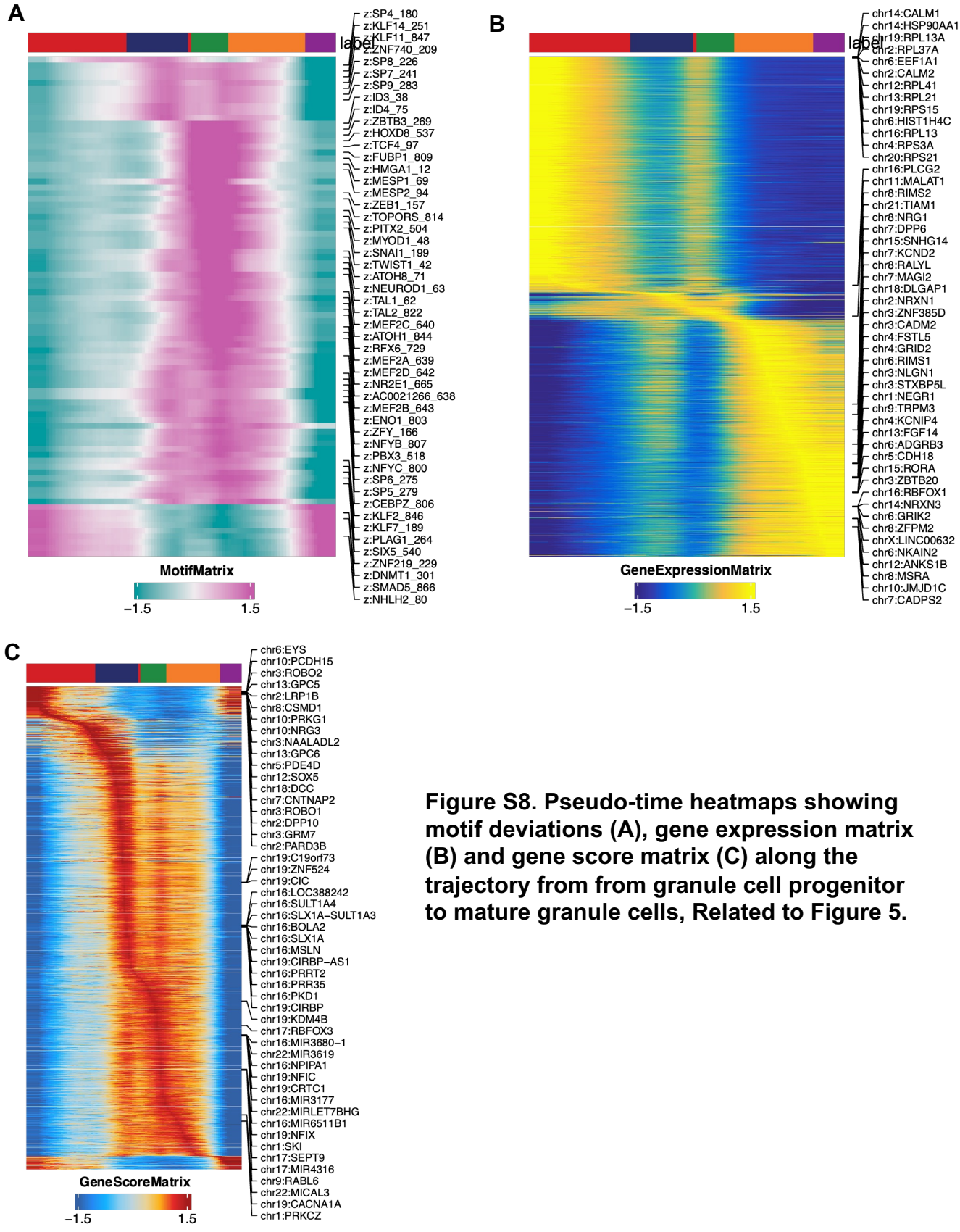

Figure S8. Pseudo-time heatmaps showing motif deviations (A), gene expression matrix (B) and gene score matrix (C) along the trajectory from from granule cell progenitor to mature granule cells, Related to Figure 5.

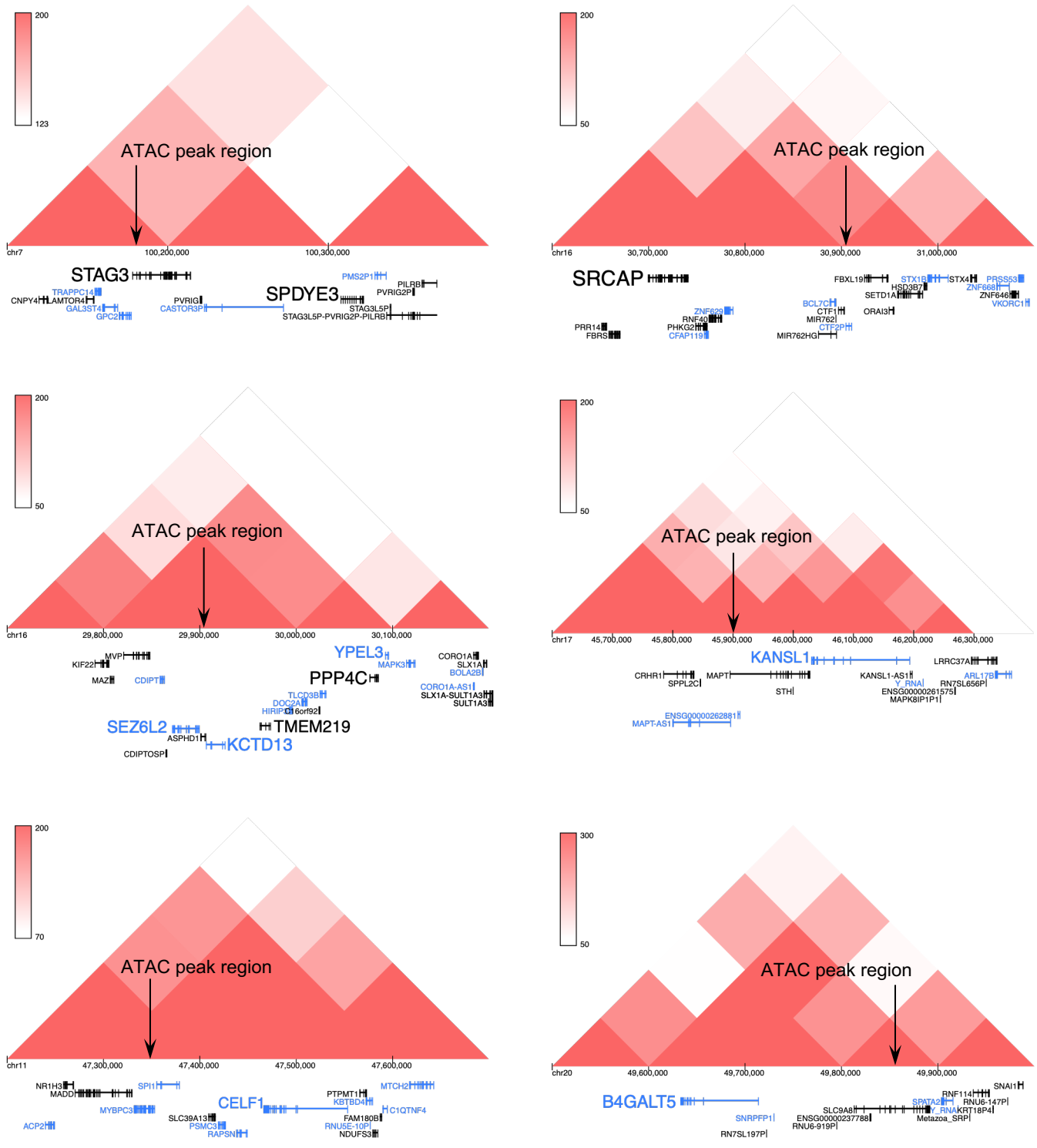

Figure S9. Published Hi-C data confirmed the regulatory relationship between candidate cis-regulatory elements and the promoters of 9 genes in human cerebellum, Related to Figure 7. Target genes are highlighted in each heatmap.

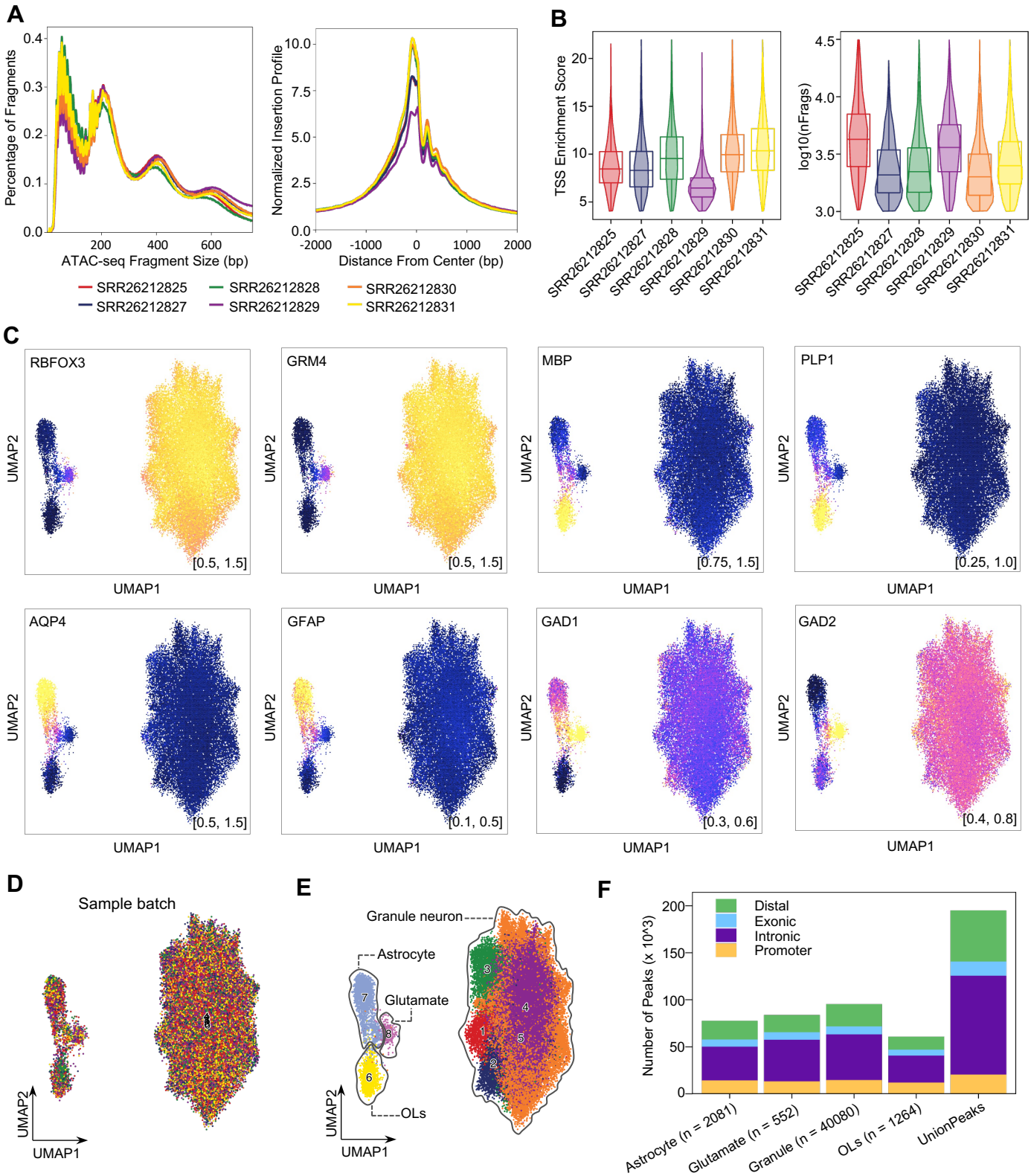

Figure S10. Analysis of snATAC-seq datasets from publicly available human aging cerebellum, Related to Figure 1. (**A**) snATAC-seq fragment size distributions and TSS enrichment profiles per sample. (**B**) Violin plots depicting the TSS enrichment score per nucleus and number of detected ATAC fragments per nucleus. (**C**) Joint UMAPs for selected marker genes colored by normalized gene activity scores. (**D**) Joint UMAP colored by sample batch. (**E**) UMAP visualization of aging brain nucleus colored by the annotated clusters. (**F**) Number of chromatin accessibility peaks for each annotated clusters as determined by snATAC-seq. Peaks were identified using ArchR.

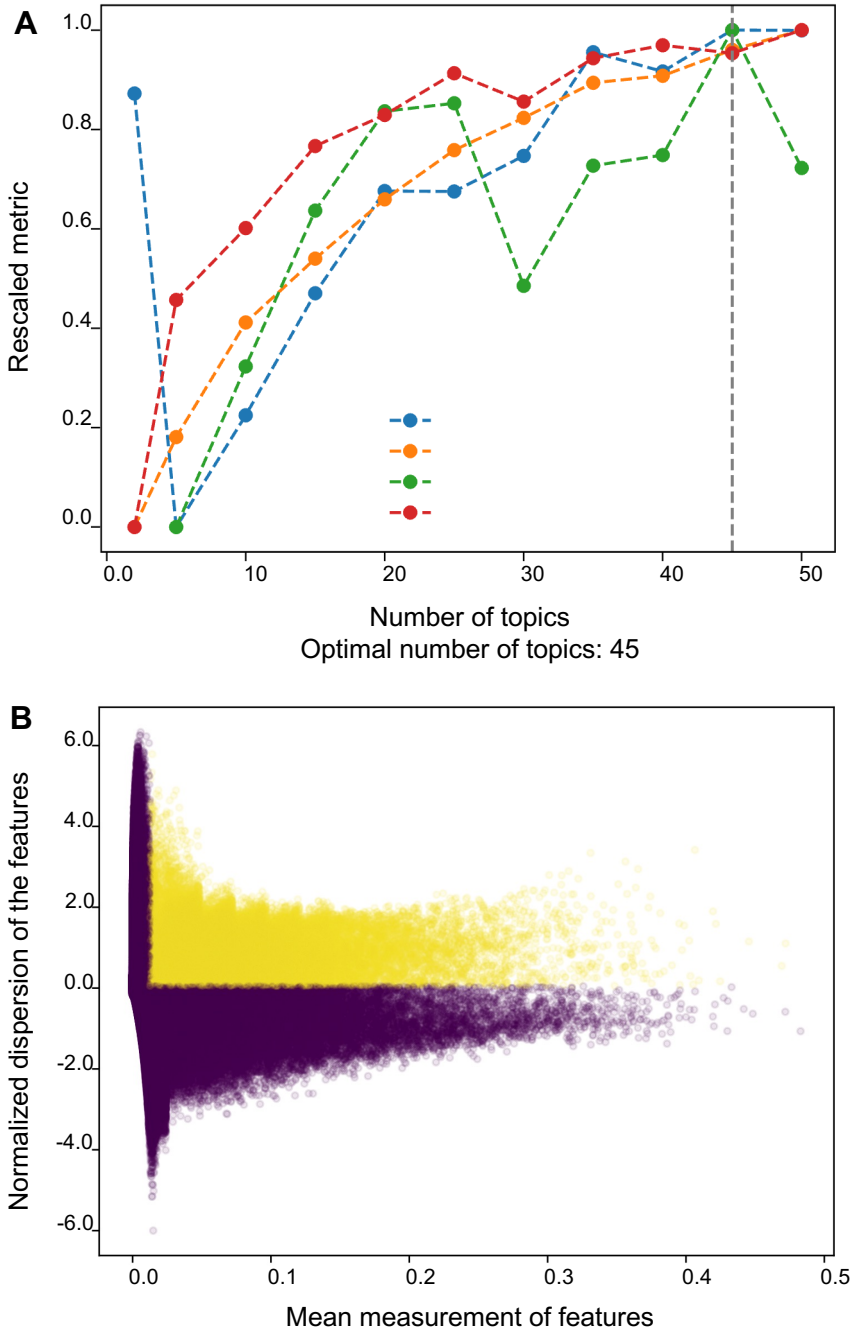

Figure S11. Analysis of enhancer candidate identification and topic modeling using pycisTopic, Related to Figure 4. (**A**) Model selection of the optimal number of topics. In this case, the optimal number of topics is 45. (**B**) Volcano plot showing highly variable regions among AD/ADRD cases and controls.